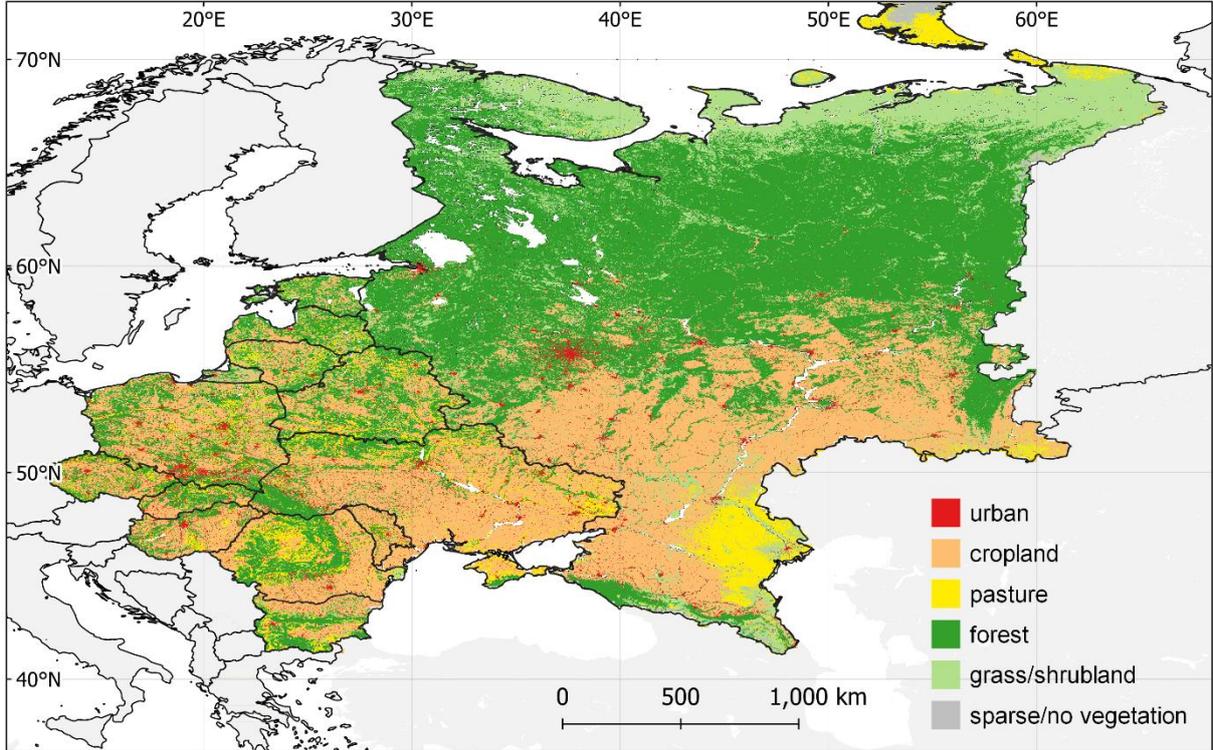
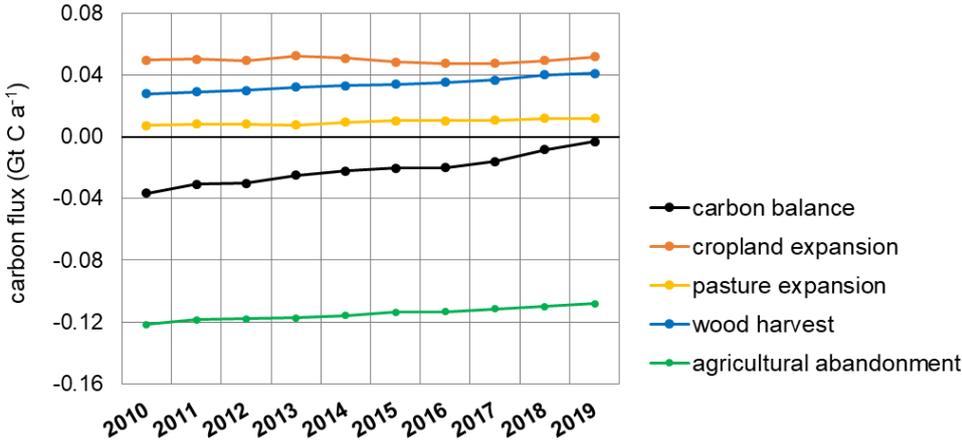


Supplementary Information

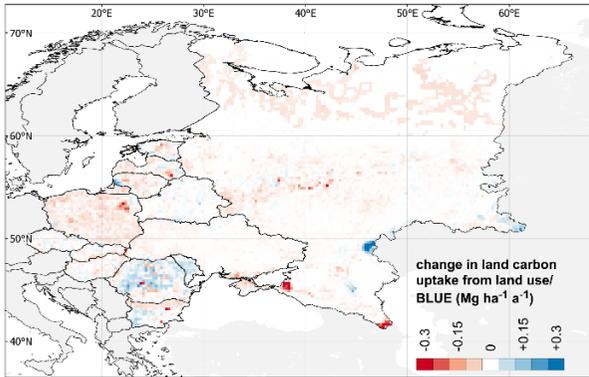


Supplementary Figure 1: Land use/cover map of Eastern Europe in 2019 based on the HILDA+ dataset ².

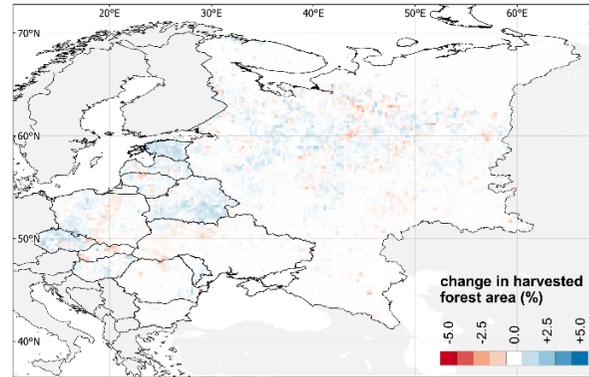


Supplementary Figure 2: Annual net carbon flux from land use change (carbon balance), derived from the BLUE model using the HILDA+ land use forcing¹, and its component fluxes from cropland and pasture change, wood harvest (net flux of release from product and slash decay and uptake by regrowth), and agricultural abandonment in Eastern Europe in 2010-2019. Negative values represent a carbon sink.

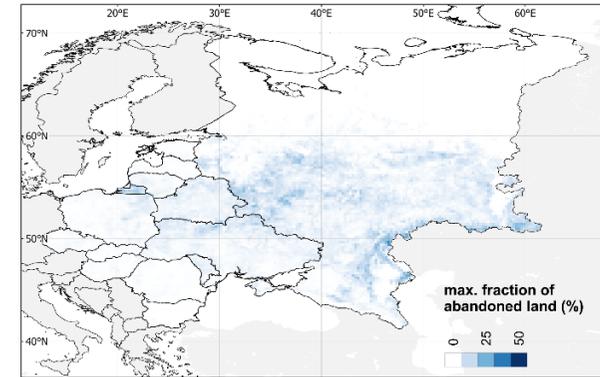
LUC: Agriculture, abandonment, harvest



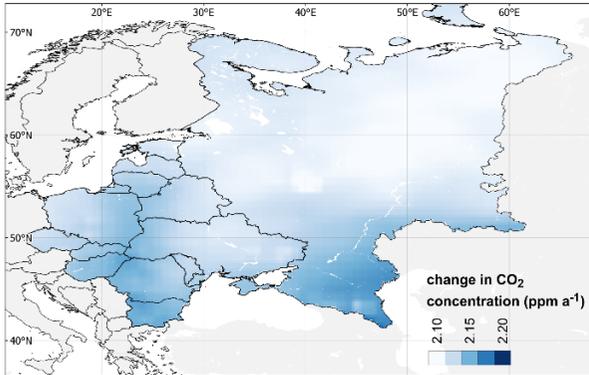
LUC: Forest harvest



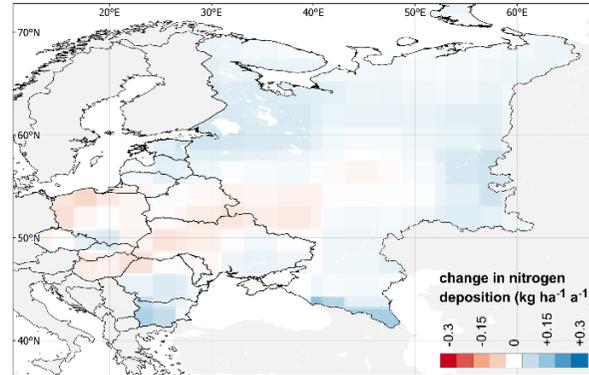
LUC: cropland abandonment



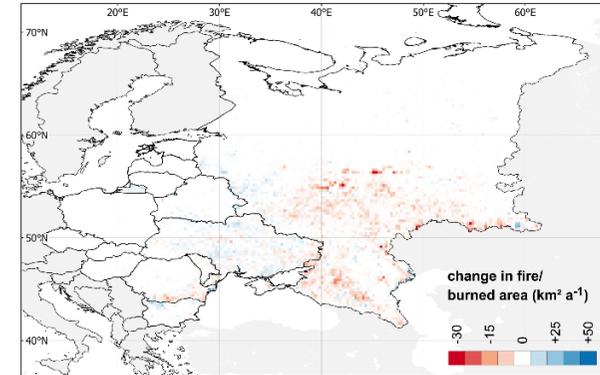
CO₂ concentration



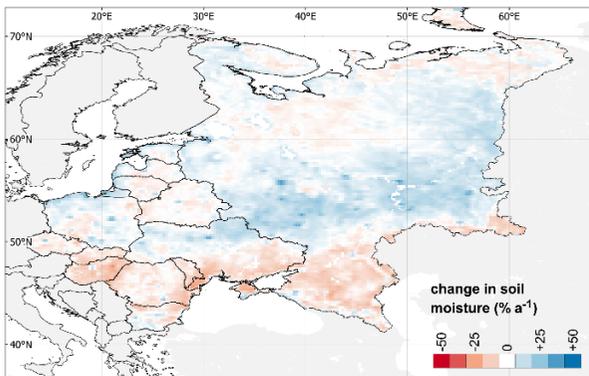
Nitrogen deposition



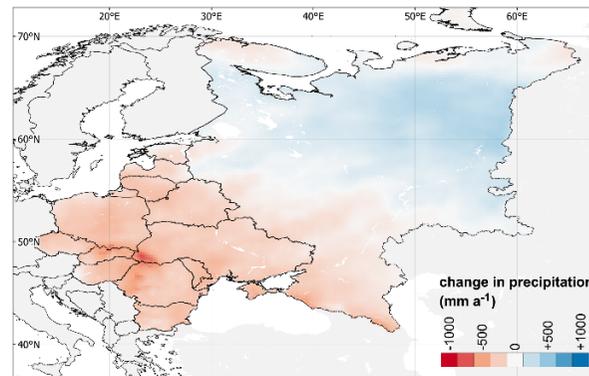
Fire



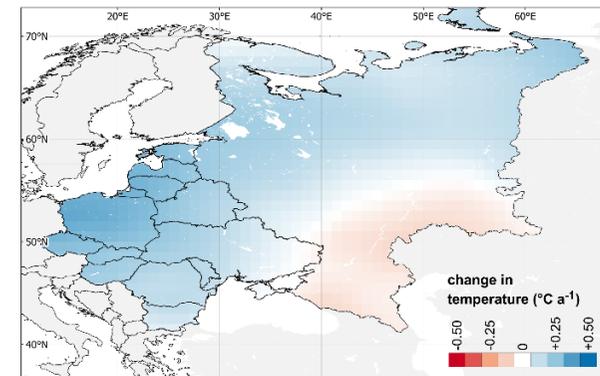
soil moisture



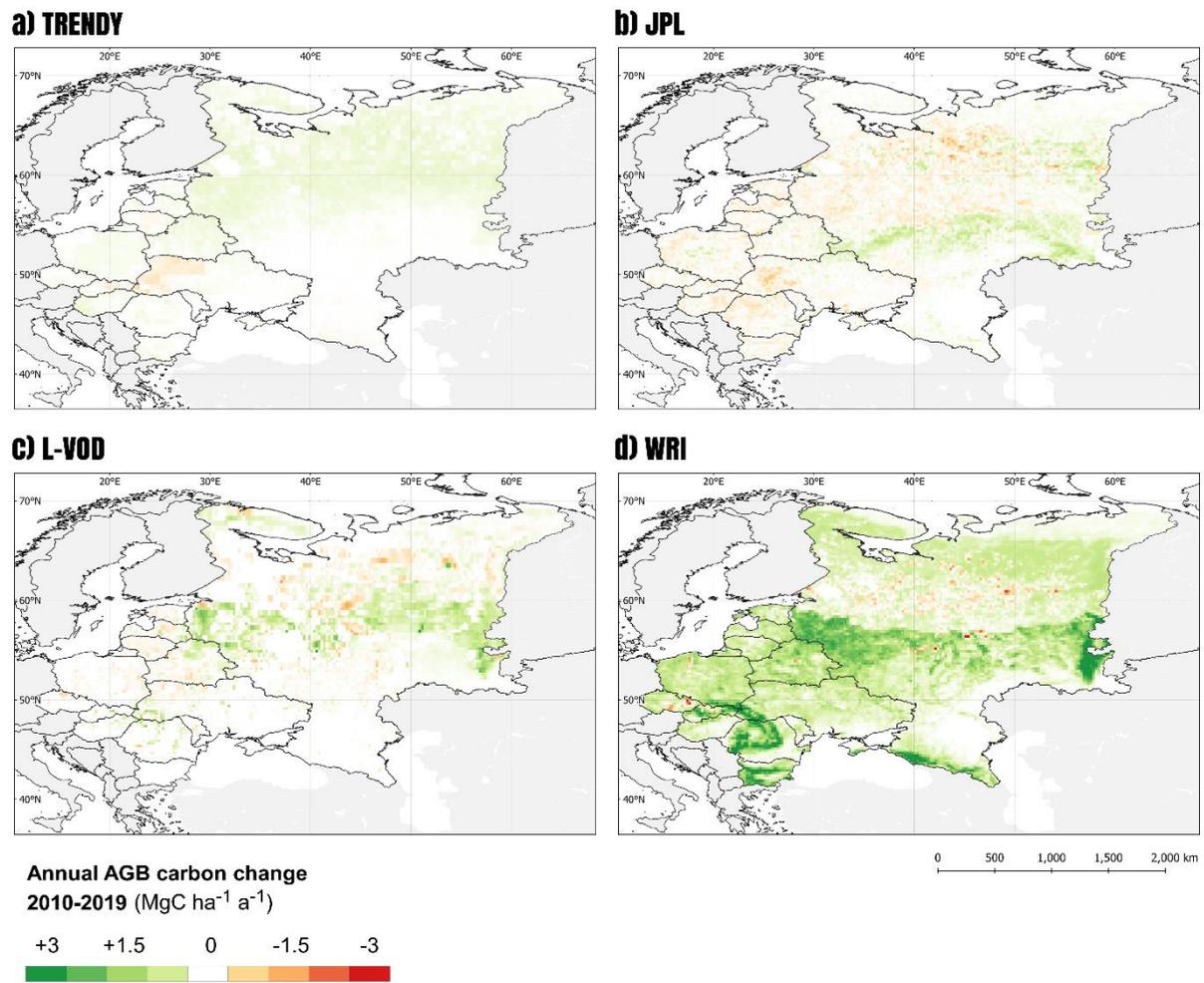
Precipitation



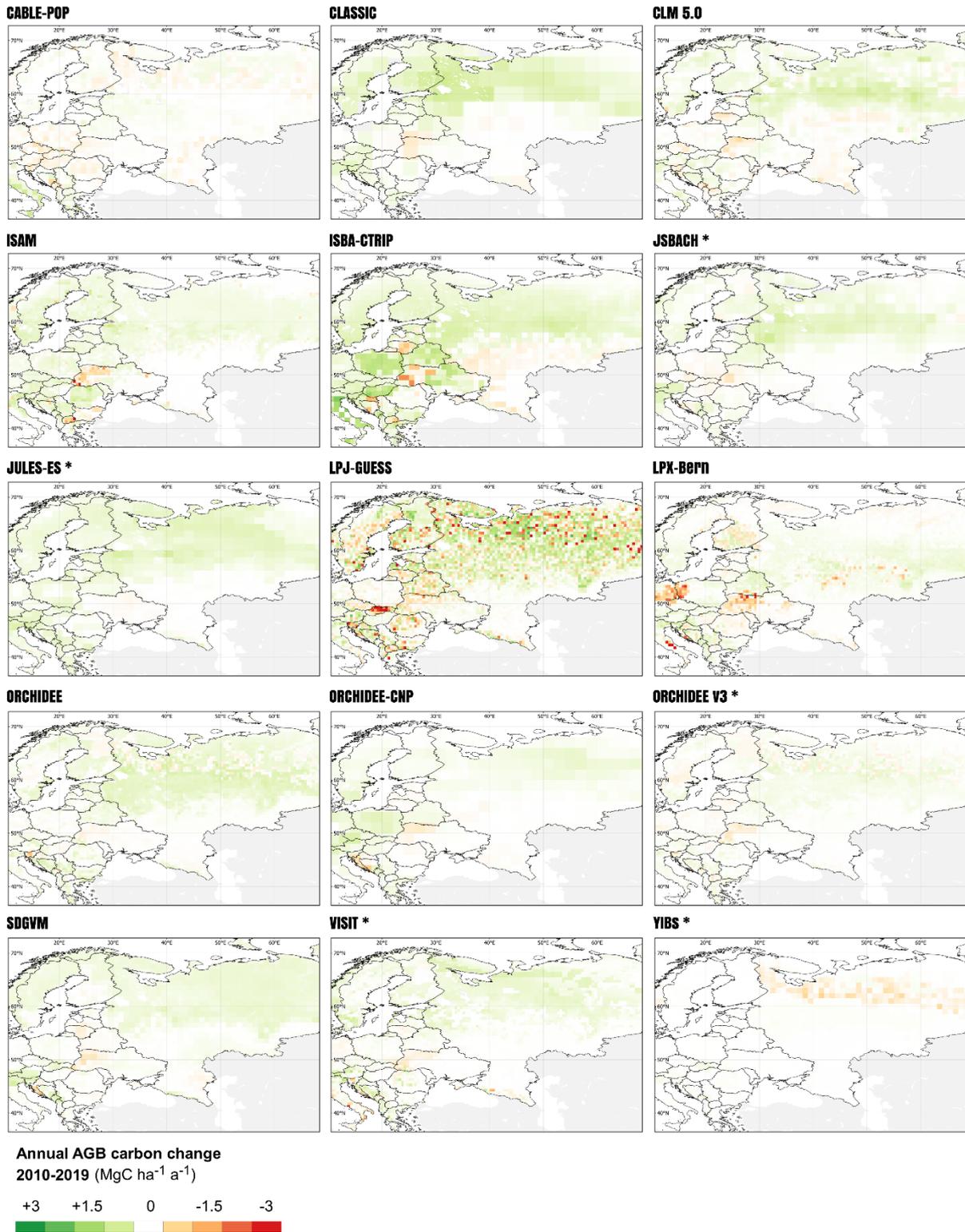
Temperature



Supplementary Figure 3: Spatial trends of possible underlying drivers and influencing factors of AGB carbon change in Eastern Europe during 2010-2019. Values are normalised to a mean value of 0 (except from cropland abandonment, which does not show change but the fraction of abandonment).

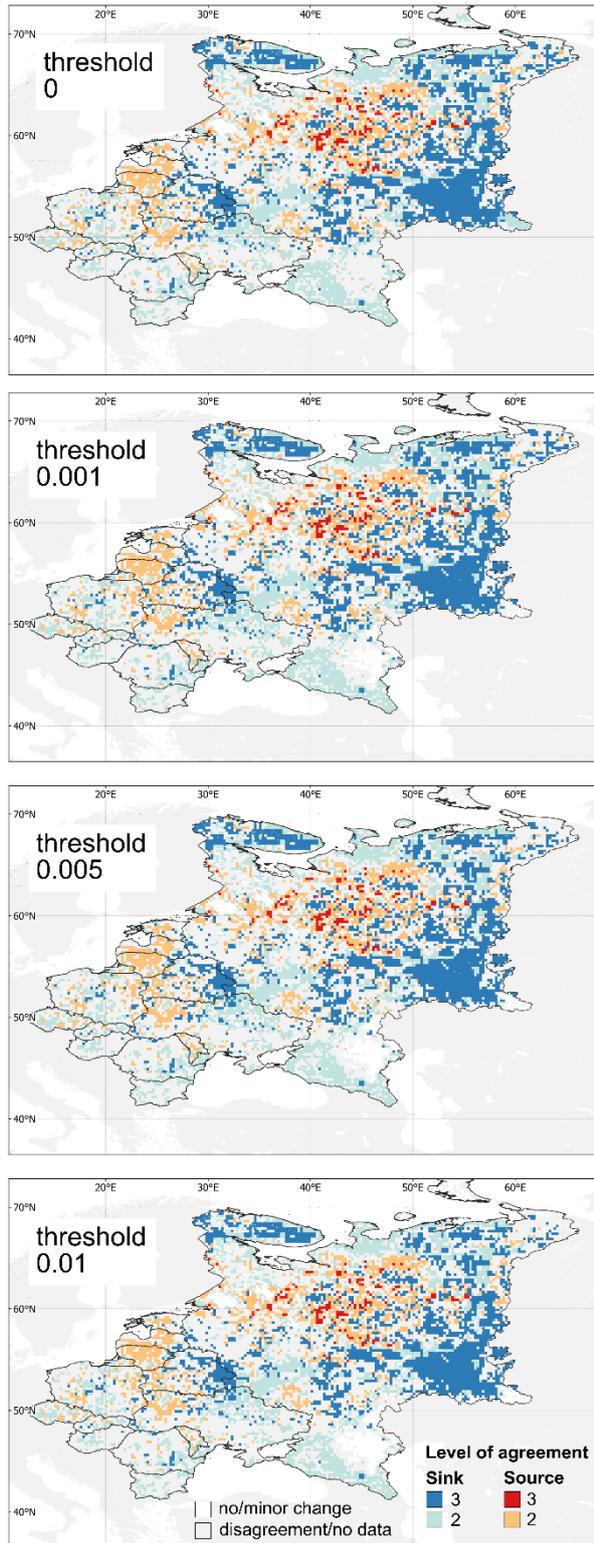


Supplementary Figure 4: Spatial patterns of carbon gains and losses in AGB (in Mg C ha⁻¹ a⁻¹) from a) TRENDY (mean of 15 models), b) JPL³, c) L-VOD⁴ and d) WRI⁵ in Eastern Europe during 2010-2019.

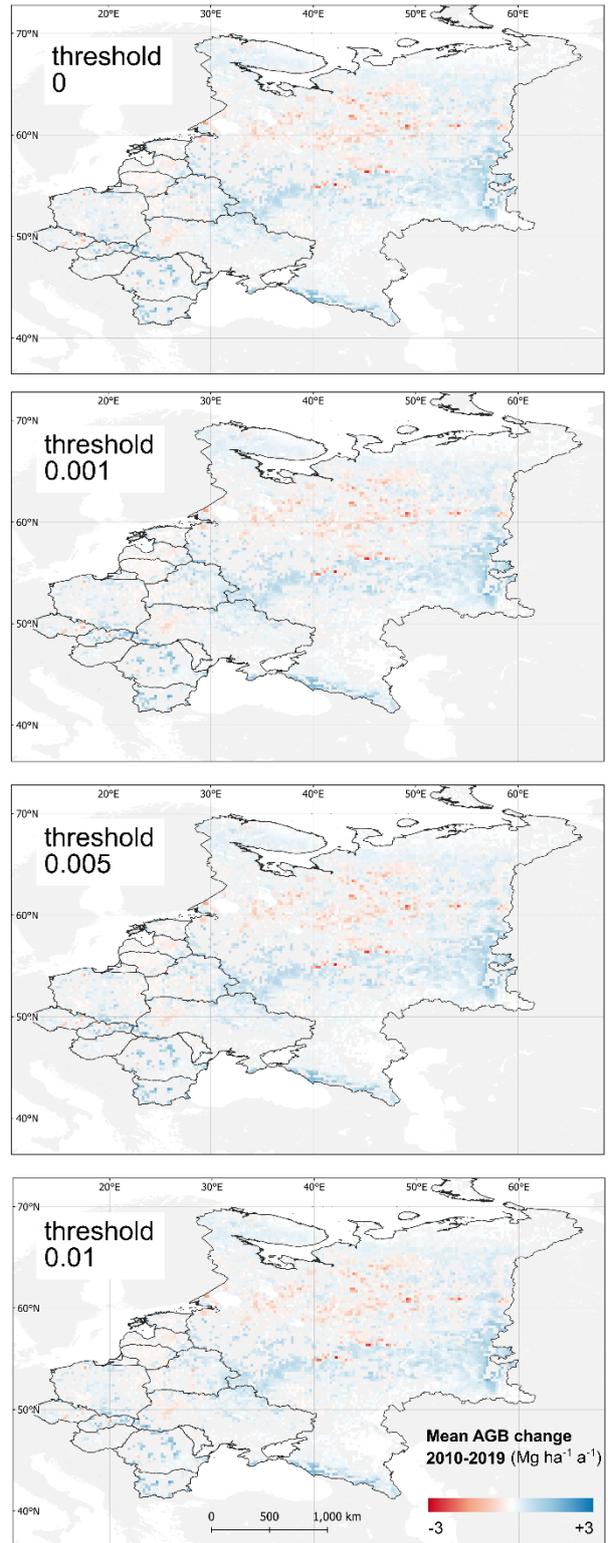


Supplementary Figure 5: Spatial patterns of AGB carbon change (in Mg C ha⁻¹ a⁻¹) in Eastern Europe during 2010-2019 from 15 TRENDY models. These models account for both land-use and environmental changes as drivers of carbon fluxes. *) Carbon in roots (cRoot) was not available for calculating the AGB carbon change, but computed from above-/below-ground biomass ratio ⁶.

Agreement

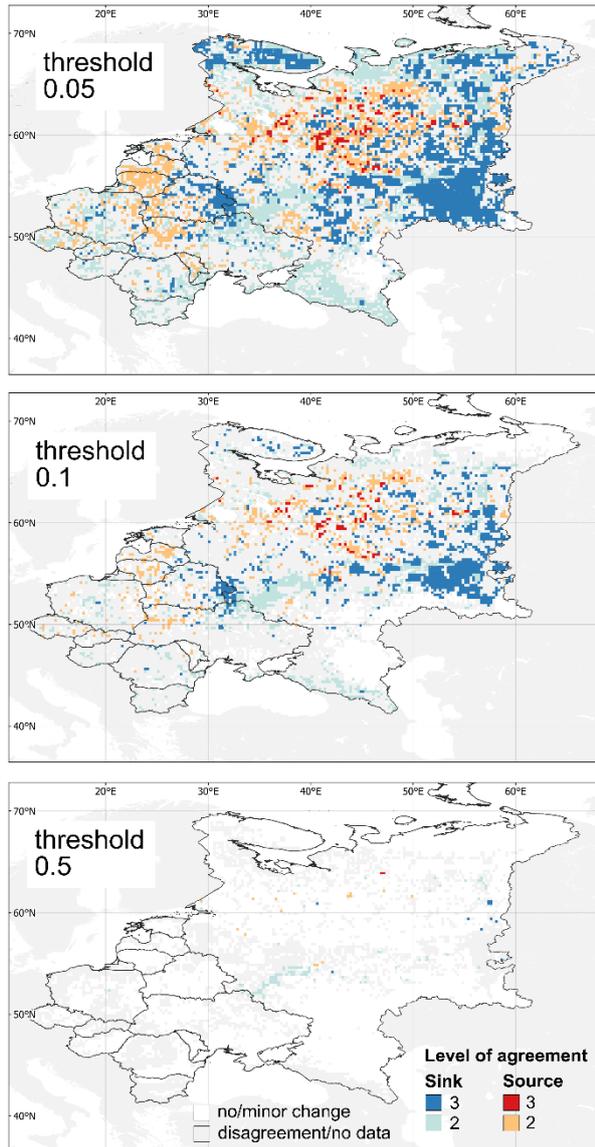


Harmonised AGB change

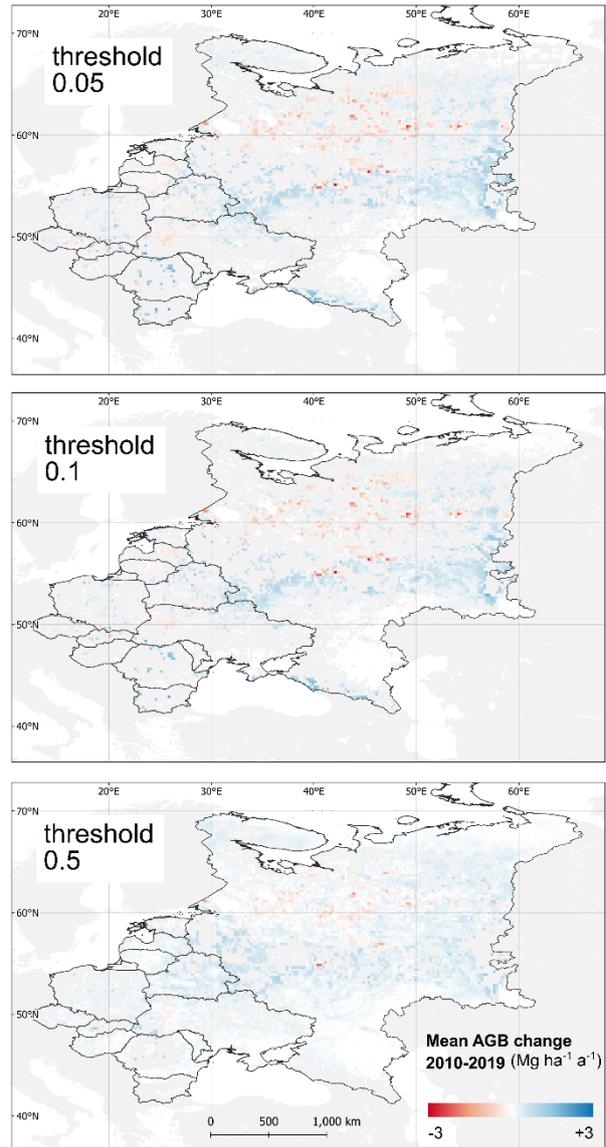


Supplementary Figure 6: Sensitivity of agreement (left column) on carbon gains (source) and losses (sink) as well as harmonised mean AGB change (right column) in Eastern Europe during 2010-2019 from three datasets (L-VOD, JPL, and WRI) to different thresholds. Sources are defined by $\Delta\text{AGB} < \text{threshold}$, sinks by $\Delta\text{AGB} > \text{threshold}$ in $\text{Mg C ha}^{-1} \text{a}^{-1}$. Levels of agreement represent the number of agreeing datasets. The harmonised mean AGB change was derived for all datasets that agree on either a carbon source or sink or no/minor change in areas with an agreement level of at least 2. Areas of disagreement are displayed in grey.

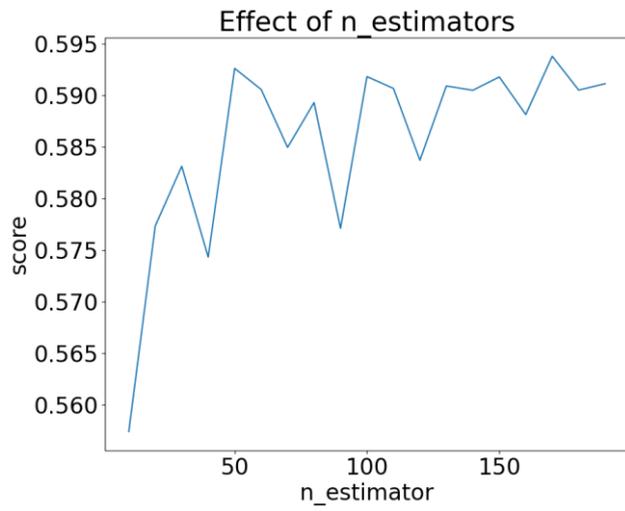
Agreement



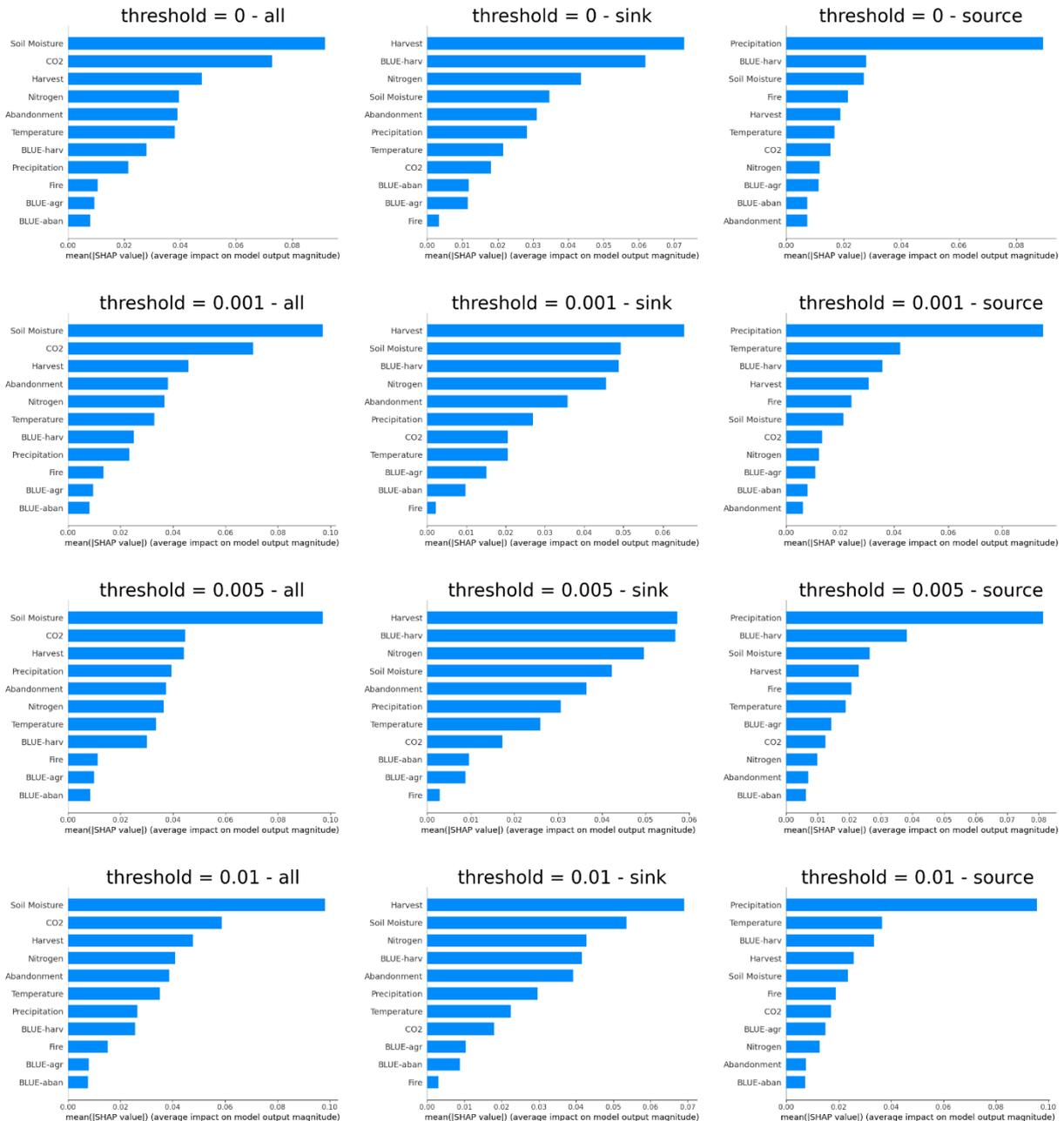
Harmonised AGB change



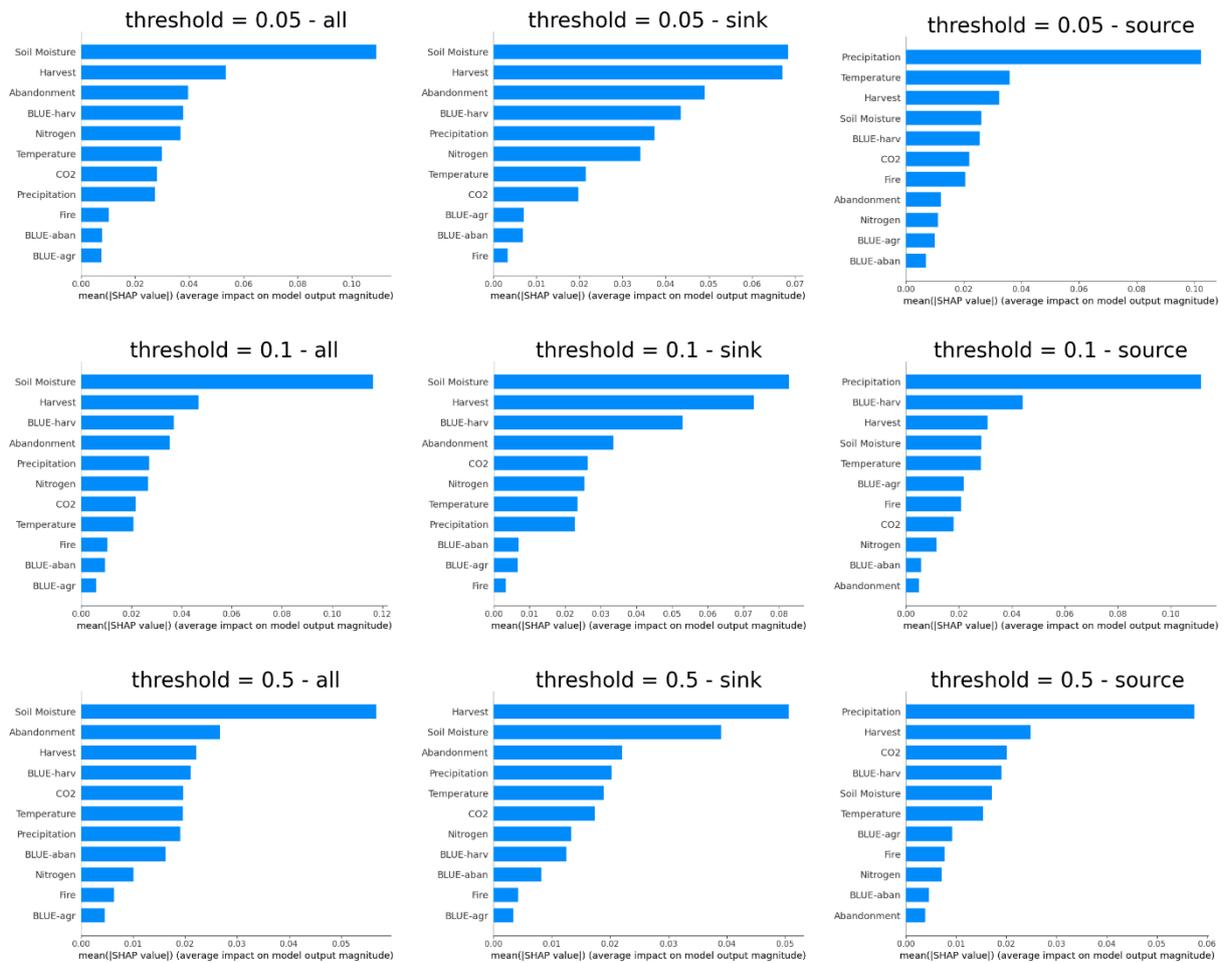
Supplementary Figure 6 (continued): Sensitivity of agreement (left column) on carbon gains (source) and losses (sink) as well as harmonised mean AGB change (right column) in Eastern Europe during 2010-2019 from three datasets (L-VOD, JPL, and WRI) to different thresholds. Sources are defined by $\Delta\text{AGB} < \text{threshold}$, sinks by $\Delta\text{AGB} > \text{threshold}$ in $\text{Mg C ha}^{-1} \text{ a}^{-1}$. Levels of agreement represent the number of agreeing datasets. The harmonised mean AGB change was derived for all datasets that agree on either a carbon source or sink or no/minor change in areas with an agreement level of at least 2. Areas of disagreement are displayed in grey.



Supplementary Figure 7: Exemplary performance analysis of a random forest regression model: the random forest model with 170 decision trees resulted in the highest score (R^2 value of around 0.592 for the test set). Here, all grid cells of AGB carbon change were taken into account (subset 3).



Supplementary Figure 8: Sensitivity of driver analysis in form of feature importance based on average Shapley values from random forest regression to different thresholds of AGB carbon change. Thresholds were applied to derive the harmonised mean AGB change from three datasets (L-VOD, JPL, and WRI), which was used as a response variable for random forest regression. Random forest regression was applied to three different subsets: all (overall AGB carbon change), sink (AGB carbon sink areas only), source (AGB carbon source areas only), see Table S5 for model performance and sample sizes.



Supplementary Figure 8 (continued): Sensitivity of driver analysis in form of feature importance based on average Shapley values from random forest regression to different thresholds of AGB carbon change. Thresholds were applied to derive the harmonised mean AGB carbon change from three datasets (L-VOD, JPL, and WRI), which was used as a response variable for random forest regression.

Supplementary Table 1: List of European subregions (in bold) and included countries.

Region	North	West	South	East
Countries included	Denmark Finland Sweden Norway	Austria Belgium France Ireland Germany Liechtenstein Luxembourg Netherlands Switzerland United Kingdom	Albania Bosnia and Herzegovina Croatia Greece Kosovo Macedonia Montenegro Italy Portugal Serbia Slovenia Spain	Belarus Bulgaria Czechia Hungary Estonia Latvia Moldova Lithuania Poland Romania Slovakia Ukraine
				European Russia (Eastern border: Ural Mountains)

EE: East + Russia

Supplementary Table 2: Standard deviations (as variability across time) of average land above-ground biomass (AGB) carbon flux (in Gt C a⁻¹) from different datasets (see Table 1, Table 2 and Figure 2 in the main paper) for European regions.

Data	SURF	GOSAT	OCO2	L-VOD	JPL **	WRI **	UNFCCC	BLUE[°] **
Period	2010-18	2010-15	2015-18	2010-19	2010-2019	2010-19	2010-19	2010-19
North	0.031	0.022	0.013	-0.003	0.042	0.022	0.009	0.001
West	0.059	0.115	0.033	0.018	0.014	0.032	0.005	0.007
South	0.033	0.050	0.024	0.007	0.035	0.030	0.012	0.010
East	0.111	0.097	0.063	0.016	0.085	0.039	0.005	0.008
Russia	0.218	0.127	0.053	0.083	0.065	0.065	0.003	0.005
EE	0.105	0.088	0.036	0.099	0.079	0.103	0.127	0.013
Europe	0.081	0.088	0.042	0.127	0.170	0.187	0.064	0.028

[°] includes AGB, below-ground biomass (BGB) and soil organic carbon (SOC)

** refers to gross carbon sink estimates.

Supplementary Table 3: Average net land above-ground biomass (AGB) carbon flux (in Gt C a⁻¹) from different datasets (see Table 1 and Figure 2 in the main paper) for European regions.

Data	SURF	GOSAT	OCO2	L-VOD	JPL	WRI	UNFCCC	BLUE[°]
Period	2010-18	2010-15	2015-18	2010-19	2010-19	2010-19	2010-19	2010-19
North	-0.08	-0.07	0.02	0.02	-0.01	-0.07	-0.07	0.01
West	-0.20	-0.17	0.04	-0.08	0.00	-0.13	-0.06	-0.01
South	-0.09	0.01	0.04	-0.07	0.01	-0.11	-0.10	-0.02
East	-0.09	-0.17	-0.09	-0.04	0.01	-0.15	-0.16	-0.03
Russia	-0.44	-0.33	-0.22	-0.41	-0.02	-0.21	-0.04	0.01
EE	-0.53	-0.50	-0.32	-0.45	-0.01	-0.36	-0.20	-0.02
EE share	59%	68%	143%	77%	140%	54%	47%	53%
Europe	-0.89	-0.73	-0.22	-0.59	-0.01	-0.66	-0.44	-0.04

[°] includes AGB, below-ground biomass (BGB) and soil organic carbon (SOC)

Supplementary Table 4: Hypothesised relationship between change of driver indicators and AGB carbon change, either sink (positive AGB change) or source (negative AGB change). Negative relations are displayed as -, positive relations are displayed as +, unclear relations are displayed as +/-.

Driver indicator	Relation to AGB carbon sink	Relation to AGB carbon source	Description and reference
BLUE-agr	-	+	Agricultural expansion leads to enhanced carbon emissions (carbon source) ^{7,8} .
BLUE-aban	+	-	Agricultural land abandonment leads to enhanced woody biomass (carbon sink) ^{7,9,10} .
BLUE-harv	-	+	Wood harvest removes biomass (carbon source) ⁸ .
Harvest	-	+	see <i>BLUE-harv</i>
Abandonment _{fraction}	+	-	see <i>BLUE-aban</i>
Fire	-	+	Fires lead to biomass removal and enhanced carbon emissions (carbon source) ¹¹ .
Soil moisture	+/-	+/-	Unclear relation ¹²
Precipitation	+/-	+/-	Unclear relation ¹²
Temperature	+/-	+/-	Unclear relation ¹²
CO ₂	+	-	CO ₂ fertilization effect enhances biomass production (carbon sink) ^{13,14} .
Nitrogen	+	-	Nitrogen deposition enhances biomass production (carbon sink) ¹⁴ .

Supplementary Table 5: Sensitivity of random forest regression to different thresholds of AGB carbon change for different subsets. Thresholds were applied to derive the harmonised mean AGB change from three datasets (L-VOD, JPL, and WRI), which was used as a response variable for random forest regression. N: number of pixels used (training plus test data), R²: R-Squared/model performance, RMSE: root-mean-square error.

Subset: Overall AGB carbon change (both carbon sinks and sources)

Threshold	0	0.001	0.005	0.01	0.05	0.1	0.5
N	7086	7097	6965	6786	5689	5309	9373
R²	0.56	0.56	0.59	0.6	0.59	0.55	0.52
RMSE	27%	26%	26%	27%	27%	25%	14%

Subset: AGB carbon sink (harmonised AGB carbon change > 0)

Threshold	0	0.001	0.005	0.01	0.05	0.1	0.5
N	5279	5224	5130	4983	4274	4182	8147
R²	0.75	0.75	0.77	0.75	0.78	0.76	0.62
RMSE	15%	15%	14%	15%	14%	15%	11%

Subset: AGB carbon source (harmonised AGB carbon change > 0)

Threshold	0	0.001	0.005	0.01	0.05	0.1	0.5
N	1807	1811	1773	1742	1353	1065	1164
R²	0.44	0.32	0.36	0.48	0.44	0.45	0.39
RMSE	20%	24%	19%	21%	24%	24%	14%

Supplementary references

1. Ganzenmüller, R. *et al.* Land-use change emissions based on high-resolution activity data substantially lower than previously estimated. *Environ. Res. Lett.* **17**, 064050 (2022).
2. Winkler, K., Fuchs, R., Rounsevell, M. & Herold, M. Global land use changes are four times greater than previously estimated. *Nat Commun* **12**, 2501 (2021).
3. Xu, L. *et al.* Changes in global terrestrial live biomass over the 21st century. *Science Advances* **7**, eabe9829 (2021).
4. INRAE BORDAEUX. INRAE BORDEAUX Soil Moisture and Vegetation products. <https://ib.remote-sensing.inrae.fr/>.
5. Harris, N. L. *et al.* Global maps of twenty-first century forest carbon fluxes. *Nature Climate Change* 1–7 (2021) doi:10.1038/s41558-020-00976-6.
6. Spawn, S. A., Sullivan, C. C., Lark, T. J. & Gibbs, H. K. Harmonized global maps of above and belowground biomass carbon density in the year 2010. *Sci Data* **7**, 112 (2020).
7. Friedlingstein, P. *et al.* Global Carbon Budget 2021. *Earth System Science Data* **14**, 1917–2005 (2022).
8. Houghton, R. A. & Nassikas, A. A. Global and regional fluxes of carbon from land use and land cover change 1850–2015. *Global Biogeochemical Cycles* **31**, 456–472 (2017).
9. Schierhorn, F. *et al.* Post-Soviet cropland abandonment and carbon sequestration in European Russia, Ukraine, and Belarus. *Global Biogeochemical Cycles* **27**, 1175–1185 (2013).
10. Fuchs, R. *et al.* Assessing the influence of historic net and gross land changes on the carbon fluxes of Europe. *Global Change Biology* **22**, 2526–2539 (2016).
11. Pilli, R., Grassi, G., Kurz, W. A., Fiorese, G. & Cescatti, A. The European forest sector: past and future carbon budget and fluxes under different management scenarios. *Biogeosciences* **14**, 2387–2405 (2017).
12. Humphrey, V. *et al.* Soil moisture–atmosphere feedback dominates land carbon uptake variability. *Nature* **592**, 65–69 (2021).
13. Wang, S. *et al.* Recent global decline of CO₂ fertilization effects on vegetation photosynthesis. *Science* **370**, 1295–1300 (2020).
14. Tharammal, T., Bala, G., Devaraju, N. & Nemani, R. A review of the major drivers of the terrestrial carbon uptake: model-based assessments, consensus, and uncertainties. *Environ. Res. Lett.* **14**, 093005 (2019).